AIChE

Modeling Cell Adhesion to a Substrate with Gradient in Ligand Density

Alireza S. Sarvestani and Esmaiel Jabbari
Biomimetic Materials and Tissue Engineering Laboratories, Dept. of Chemical Engineering, University of South Carolina, Columbia, SC 29208

DOI 10.1002/aic.11908
Published online July 31, 2009 in Wiley InterScience (www.interscience.wiley.com).

Surface density profile of bioadhesive ligands greatly influences spreading and migration of cells on substrates. A 1D peeling model is developed to predict the equilibrium adhesion strength and peeling tension of a cell membrane, adhered on a substrate with linearly increasing density of ligands. Cell membrane is modeled as a linear elastic shell subjected to a tensile force applied at the free extremity and adhesive traction due to specific receptor-ligand interactions with the substrate. Membrane peeling tension increased with gradient slope and reached an asymptotic limit independent of gradient slope but proportional to receptor-ligand interaction energy. Peeling tension from substrates with negative gradient slope, at the rear edge of adhesion zone, was considerably lower than the tension from substrates with positive gradient slope at the leading edge, indicating that detachment is more likely to be initiated at the rear edge. This prediction leads to a possible mechanism for experimentally observed haptotactic locomotion of motile cells toward the direction of higher ligand density.
 AIChE J, 55: 2966–2972, 2009
Keywords: cell adhesion, mathematical modeling, ligand gradient, ligand-receptor interaction energy, cell locomotion

Introduction

Cell-substrate interactions play a central role in regulation of cellular functions such as adhesion, locomotion, growth, proliferation, and differentiation.[1–5] These interactions typically occur between heterodimeric integrin receptors present on the cell surface and ligands attached to the components of extracellular matrix (ECM). Ligands are specific functional domains of ECM proteins, such as fibronectin, laminin, vitronectin, and collagen, with binding affinity toward integrin receptors.[6–8] Cell adhesion responds to a wide range of physical and chemical cues from the surrounding matrix. Surface properties including surface energy, roughness, and chemical structure can influence protein adsorption and modulate cell motility.[9–11] This regulatory effect of substrate on cell motility has been used to design novel biomaterials with the ability to guide cell migration, proliferation, morphogenesis, and to control cell-biomaterial interactions.[12,13]

Surface density of bioadhesive ligands has been shown to greatly influence spreading and migration of cells on substrates. In particular, substrates with gradient patterns of ligand density are widely used for guiding cell migration on biomaterials. Micropatterning techniques with UV radiation,[14,15] electrochemical reactions,[16] plasma polymerization,[17,18] microfluidic-based systems,[19,20] and photolithography[21,22] have been used to produce surface-grafted gradient of peptides and proteins on substrates. Studies have demonstrated that cells preferentially move toward regions of increasing adhesiveness.[23–28]

Despite extensive experimental studies, quantitative models to predict the equilibrium aspects of cell adhesion on a substrate with gradient in ligand density are rare. Existing models describing thermodynamics of cell adhesion are based on uniform distribution of surface ligands. Accordingly, two major classes of deterministic models,

Correspondence concerning this article should be addressed to E. Jabbari at jabbari@engr.sc.edu
Current Address of Alireza S. Sarvestani: Dept. of Mechanical Engineering, University of Maine, Orono ME 04469.

thermodynamic and kinetic, for receptor-ligand mediated cell adhesion have been developed. Equilibrium models predict the strength of adhesion, interfacial contact area, and the force necessary to disrupt adhesion to the substrate, as a function of receptor and ligand properties and mechanics of the cell.[29–31] Kinetic models describe cell adhesion in terms of the kinetics equations for the interactions between membrane receptors and substrate ligands and the nonequilibrium nucleation and growth processes.[32,33]

Previously, we proposed a model to analyze the kinetics of membrane adhesion on substrates with linearly increasing density of immobilized ligands.[34] The model was able to predict the time-dependent displacement of the adhesion front in terms of receptor density, receptor mobility, and the dynamics of receptor-ligand interaction between the cell membrane and substrate. In this work, the focus is on the equilibrium aspect of cell adhesion in response to a gradient in ligand density on a solid substrate. Employing the methodology developed by Evans and Dembo et al.,[30,35] a 1D membrane peeling model is developed to predict the equilibrium adhesion strength and peeling tension of the cell membrane with respect to a gradient in ligand density on a substrate. The model includes the kinetics of noncovalent receptor-ligand interactions and the effect of external stimuli on deformation of the cell membrane. The objective is to understand, using a peeling model, how the attachment strength of the membrane to the substrate is regulated by the gradient in ligand density.

Model Development

Figure 1 represents geometry of the 1D peeling model considered in this work. The position along the cell membrane is described by the arc-length coordinate r, as well as Cartesian coordinates x and y. The membrane-substrate adhesion zone represents a segment of the membrane, extending from $r = 0$ to $r = r_0$, where transmembrane receptors and complementary immobilized surface ligands can specifically interact. The membrane is modeled as a linear elastic shell subjected to adhesive forces in the adhesion zone and macroscopic tension T_{mac}, arising from any applied force on the membrane. T_{mac} acts on the cell remote from the adhesion zone and at orientation determined by the macroscopic contact angle θ_{mac}. The membrane microscopic contact angle at the edge of adhesion zone (i.e., at $r = r_0$) is represented by θ_{mic}.

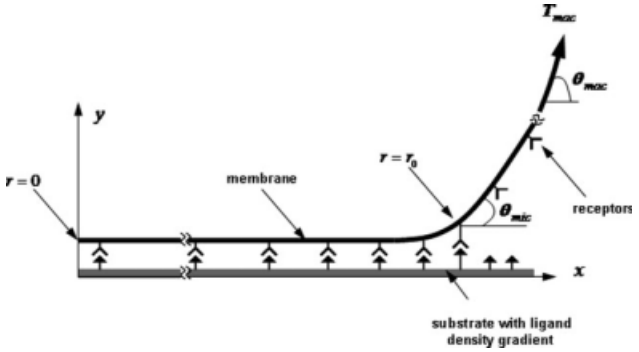

Figure 1. Geometry of the 1D peeling model for cell adhesion on a ligand gradient substrate.

The position along the membrane is defined by arc-length r and Cartesian coordinates x and y. The density of surface ligands increases linearly along the positive direction of x-axis. The adhesion zone starts from $r = r_0$ and extends to $r = 0$ along the membrane. The membrane slope at the edge of adhesion zone ($r = r_0$) is represented by the microscopic contact angle θ_{mic}. At free end of the membrane, macroscopic tension T_{mac} is applied at a specified angle θ_{mac}.

The surface density of ligands is assumed to linearly increase along the x-axis, as follows:

$$L(x) = L_0 + \beta x, \tag{1}$$

where L_0 is a constant density at $x = 0$ and β is the slope of gradient in ligand density. At steady-state, we can write a balance between the density of ligands (L), receptors (R), and ligand-receptor pairs (C) as follows:

$$k_{eq}\,(L - C)\,(R - C) - C = 0, \tag{2}$$

where k_{eq} is the equilibrium affinity constant between ligands and receptors, given by[29] the following:

$$k_{eq} = k_{eq}^0 \exp\left[-\kappa l^2 / 2k_B T\right]. \tag{3}$$

Here, k_{eq}^0 is the equilibrium constant in the force-free state, l is the bond extension beyond the force-free length, κ is the spring constant of a ligand-receptor bond, and $k_B T$ is thermal energy. Solution of Eq. 2 yields a quadratic expression for the equilibrium distribution of bonds between receptors and ligands. The resultant adhesive traction acting along receptor-ligand bonds, σ, is assumed to be normal to the membrane surface, where the magnitude of tensile force of each bond is taken to be linearly proportional to bond extension. Thus, according to Evans,[30]

$$\sigma = \frac{2\gamma l}{l_m^2}, \tag{4}$$

where l_m is the maximum possible extension before dissociation, and γ is adhesion energy. In addition, we assume that the bond distribution between ligands and receptors is continuous throughout the adhesion zone. Thus, Eq. 4 can be written as $\sigma(r = 2\gamma(r)l/l_m^2)$, where $\gamma(r) = \gamma_{ad} C(r)$ and γ_{ad} is the stored energy in a single ligand-receptor bond (note that γ has units of energy per unit length, γ_{ad} is the adhesion energy of each ligand-receptor bond, and C is the number of ligand-receptor bonds per unit membrane length).

Considering the relative cell-substrate geometry, the cell membrane can be divided into two regions for analysis: (a) adhesion zone subjected to specific membrane-substrate interactions ($r_0 \geq r \geq 0$) and (b) free macroscopic region over which adhesion is negligible ($r \geq r_0$). At equilibrium, balancing the forces and moments in each region results in

$$V(r) = -\frac{dM(r)}{dr}, \tag{5a}$$

$$\frac{dT(r)}{dr} - V(r)\rho(r) = 0, \tag{5b}$$

$$\frac{dT(r)}{dr} + T(r)\rho(r) - \sigma(r) = 0, \tag{5c}$$

Table 1. Numerical Values Used for Dimensional Parameters in the Model

Parameter	Definition	Physiological Range	Source
R	Receptor density	10^9–10^{12} cm^{-2}	[35]
L_0	Constant ligand density	10^6–10^{12} cm^{-2}	[37]
k_{eq}	Receptor-ligand affinity	10^{-10}–10^{-5} cm^2	[35]
l_m	Maximum bond extension	10–100 nm	[29]
B	Bending modulus	0.4–4×10^{-12} erg	[38]
γ_{ad}	Energy of a single bond	6–15×10^{-13} erg	[39]
κ	Spring constant	10^{-2}–10 dyn cm^{-1}	[29]

where V, M, and T are the shear force, bending moment, and tensile force in the membrane, respectively. ρ is local curvature of the membrane defined by $\rho = d\theta/dr$, where $\theta(r)$ is the local membrane angle relative to substrate. Inside adhesion zone (i.e., $r_0 \geq r \geq 0$), this angle can be related to bond extension l by[36] the following:

$$\frac{dl}{dr} = \tan\theta\left(1 + l\frac{d\theta}{dr}\right). \tag{6}$$

Since the membrane is considered to be elastic, the following constitutive relationship holds between the bending moment and curvature:

$$M(r) = B(\rho(r) - \rho_0), \tag{7}$$

where ρ_0 is the reference curvature and B is bending modulus of the membrane. Substitution of Eq. 7 into Eq. 5 results in the following equation for free macroscopic region of the membrane:

$$T = -\frac{d^2T}{d\theta^2}, \quad r \geq r_0, \tag{8}$$

which can be solved in terms of macroscopic tension (T_{mac}) and contact angle (θ_{mac}), as follows[30]:

$$T(r) = T_{mac}\cos(\theta_{mac} - \theta(r)), \quad r \geq r_0. \tag{9a}$$

Accordingly, the shear force and membrane curvature in the macroscopic region are given by the following:

$$V(r) = T_{mac}\sin(\theta_{mac} - \theta(r)), \quad r \geq r_0, \tag{9b}$$

$$(\rho(r))^2 = \frac{2T_{mac}}{B}[1 - \cos(\theta_{mac} - \theta(r)] + \rho_0^2, \quad r \geq r_0. \tag{9c}$$

To obtain the corresponding equilibrium equations in the adhesion zone, we define the following nondimensional quantities:

$$\bar{r} = \frac{r}{l_m},\ \bar{l} = \frac{l}{l_m},\ \bar{\gamma} = \frac{\gamma l_m^2}{2B},\ \overline{T} = \frac{Tl_m^2}{4B},\ \overline{V} = \frac{Vl_m^2}{4B},\ \overline{M} = \frac{Ml_m}{4B} \tag{10}$$

Substitution of these quantities into Eqs. 5 and 6 leads to the following nonlinear differential equations for the local membrane angle θ and nondimensional tension $\overline{T}$[36]

$$\frac{d^3\theta}{d\bar{r}^3} - 4\overline{T}\frac{d\theta}{d\bar{r}} + 4\bar{\gamma}\bar{l} = 0, \quad r_0 \geq r \geq 0, \tag{11a}$$

$$\frac{d\overline{T}}{d\bar{r}} + \frac{1}{4}\frac{d^2\theta}{d\bar{r}^2}\frac{d\theta}{d\bar{r}} = 0, \quad r_0 \geq r \geq 0, \tag{11b}$$

$$\frac{d\bar{l}}{d\bar{r}} - \tan\theta\left(1 + \bar{l}\frac{d\theta}{d\bar{r}}\right) = 0, \quad r_0 \geq r \geq 0. \tag{11c}$$

The corresponding boundary conditions include:
(a) continuity condition at $\bar{r} = \bar{r}_0 = r_0/l_m$

$$\begin{aligned} \theta(\bar{r}_0^-) &= \theta(\bar{r}_0^+), \quad \overline{T}(\bar{r}_0^-) = \overline{T}(\bar{r}_0^+), \\ \overline{V}(\bar{r}_0^-) &= \overline{V}(\bar{r}_0^+), \quad \overline{M}(\bar{r}_0^-) = \overline{M}(\bar{r}_0^+), \end{aligned} \tag{12a}$$

(b) peeling condition at $\bar{r} = \bar{r}_0$

$$\bar{l}(\bar{r}_0) = 1, \tag{12b}$$

and (c) asymptotic membrane morphology as $\bar{r} \to 0$

$$\bar{l}(0) = 0, \quad \theta(0) = 0. \tag{12c}$$

Solution of Eqs. 9 and 11, along with the boundary conditions (12a–c) determines the membrane configuration as well as internal forces and moments along the membrane. These equations are characterized by macroscopic contact angle (θ_{mac}), adhesion length ($\bar{r}_0$), and adhesion energy ($(\bar{\gamma})$). The solution depends on the values of $\theta(\bar{r}_0) = \theta_{mic}$ and $\overline{T}(\bar{r}_0)$ which are not known before. Hence, an iterative procedure, similar to the method described by Dembo et al.,[35] is used for the numerical solution.

Results and Discussion

Using the proposed 1D peeling model, a numerical study is performed in this section to examine how the slope of ligand density gradient affects peeling tension. Table 1 represents the values of dimensional parameters used in the numerical solution and their range of variation based on theoretical predictions or experimental measurements. The dimensionless forms of the parameters in the model are listed in Table 2. The dimensionless slope of ligand gradient, represented by δ, is the major variable in the numerical solution. All calculations are performed with $\theta_{mac} = 90^\circ$ and results were qualitatively independent from the value of this angle.

Figure 2a shows the dependence of peeling tension $\overline{T}_{mac}$ on the normalized gradient slope δ for different values of

Table 2. Dimensionless parameters

Symbol	Expression	Definition
δ	$\beta l_m/L_0$	Dimensionless slope of gradient in ligand density
ω	$k_{eq}L_0$	Dimensionless ligand-receptor affinity
ϕ	$\gamma_{ad}l_m^2L_0/B$	Dimensionless adhesion energy of each ligand-receptor bond
ε	R/l_0	Receptor density/constant ligand density
μ	C/L_0	Bond density/constant ligand density
χ	$\kappa l_m^2/2k_BT$	Dimensionless spring constant

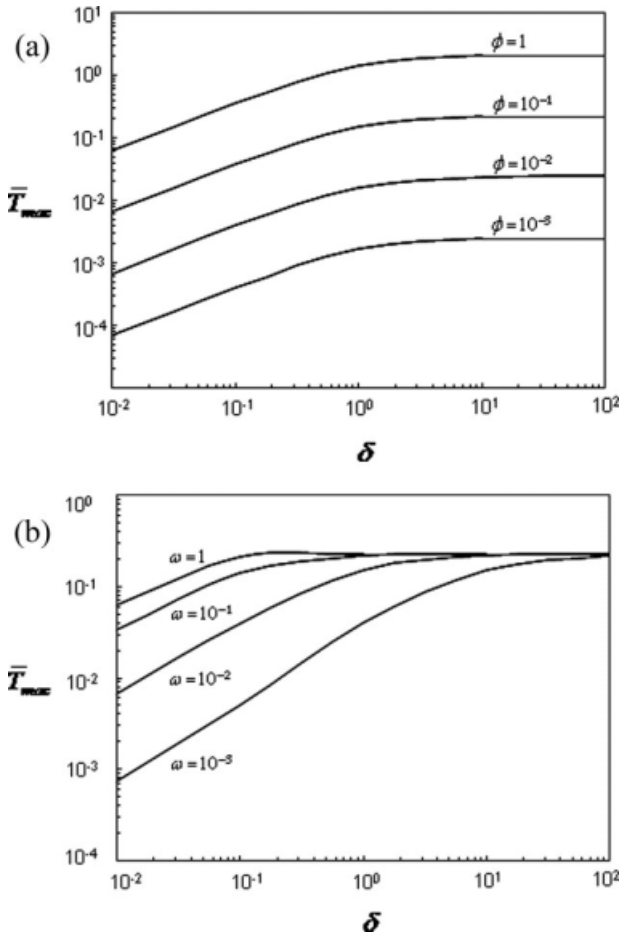

Figure 2. (a) Variation of macroscopic peeling tension ($\bar{T}_{mac}$) with the slope of ligand density gradient (δ) for different values of receptor-ligand adhesion energy (ϕ) with parameter values of $\varepsilon = 0.01$, $\omega = 0.01$, $\bar{r}_0 = 200$, and $\theta_{mac} = 90^\circ$; (b) Macroscopic peeling tension as a function of gradient slope for different values of receptor-ligand affinity (ω) with parameter values of $\phi = 0.01$, $\omega = 0.1$, $\chi = 1$, $\bar{r}_0 = 200$, and $\theta_{mac} = 90^\circ$.

ligand-receptor adhesion energy (ϕ). When δ is low, the peeling tension increases with the slope of ligand gradient. With increasing gradient slope, $\overline{T}_{mac}$ reaches an asymptotic limit, independent of the slope of gradient but proportional to adhesion energy ϕ. The effect of receptor-ligand affinity, presented by nondimensional parameter ω, on membrane peeling tension is shown in Figure 2b. The peeling tension is proportional to ligand-receptor affinity at low slopes and independent of the affinity at high-gradient slopes.

The dependence of peeling tension on ligand gradient, as shown in Figures 2a, b, is controlled by variation in the relative number of ligands and receptors at the edge of adhesion zone, thereby changing the adhesion strength. At low-gradient slopes (or equivalently low number of ligands within the adhesion zone), virtually all ligands interact with transmembrane receptors. Under that condition, increasing ligand population by increasing gradient slope enhances the adhesion strength and formation of higher ligand-receptor bonds. Above a certain value of gradient slope, the number of adhesive ligands at the edge of adhesion zone is in excess of membrane receptors; hence, the adhesion strength is not appreciably affected by increasing δ. The emergence of such transition from ligand-limited to receptor-limited regime is represented more clearly in Figure 3. According to this figure, there exists a limiting value for peeling tension which is asymptotically approached by increasing the slope of ligand gradient (δ) or lowering the expression of cell surface receptors (ε).

The bond extension profiles at the boundary layer region of the adhesion zone for different slopes of ligand gradient are shown in Figure 4a. These profiles represent the extent to which the ligand-receptor bonds are stretched which can be related to the force that the membrane exerts on each ligand-receptor bond (Eq. 4). After showing a damped oscillation-like trajectory, membrane assumes an asymptotic horizontal configuration. For membranes adhered on substrates with large δ, bond extension profile sharply approaches zero with decreasing arc-length $\bar{r}$ and curves into a domain where ligand-receptor bonds are compressed ($\bar{l} < 0$). As described by Dembo et al.,[35] appearance of a compressive domain in the bond extension profile is due to bending stiffness of the membrane which overshoots the equilibrium separation. Furthermore, according to Figure 4a, the marginal slope of membrane profile at the edge of adhesion zone (i.e., θ_{mic}) decreases with decreasing the ligand gradient slope. Consequently, the compressive strain region commences at distances farther away from the free boundary at lower gradient slopes, and higher number of ligand-receptor bonds is stretched at the onset of detachment from the substrate.

Figure 4b shows the spatial variation of ligand-receptor bond density (shown by dimensionless parameter μ) along the membrane for different values of gradient slope δ. When δ is low, bond density increases almost linearly toward the edge of adhesion zone, concurrent with linear enhancement of local ligand density. On substrates with high-ligand gradient ($\delta = 100$), local density of surface ligands exceeds the

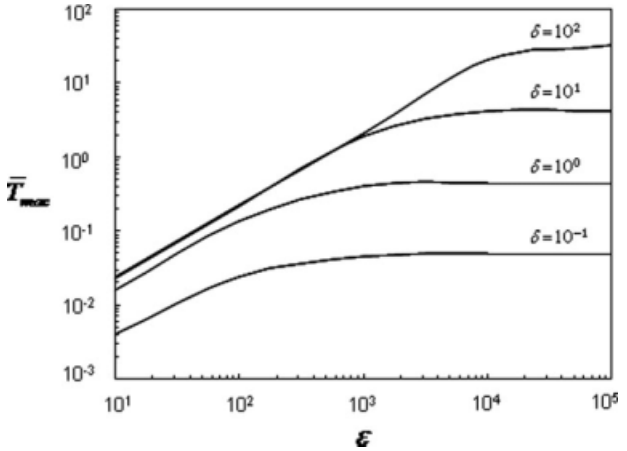

Figure 3. Dependence of macroscopic peeling tension ($\bar{T}_{mac}$) on the number density of membrane receptors.

Parameter values are $\phi = 0.1$, $\varepsilon = 0.01$, $\chi = 1$, $\bar{r}_0 = 200$, and $\theta_{mac} = 90^\circ$.

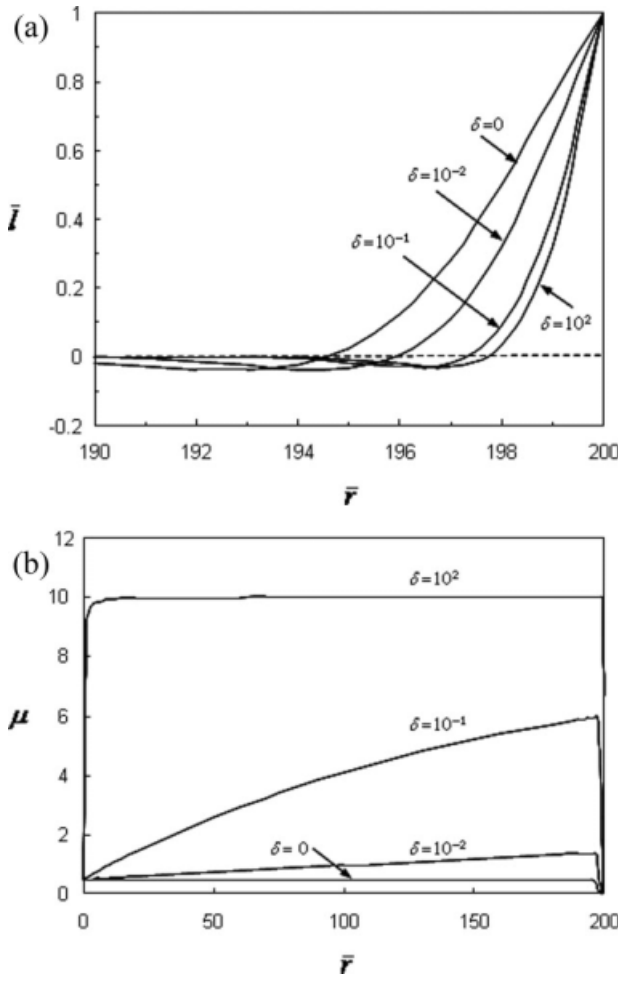

Figure 4. Spatial variation of (a) membrane deflection and (b) bond density along the adhesion zone.

Profiles are presented for different ligand gradient slopes. Parameter values are $\phi = 0.1$, $\varepsilon = 10$, $\omega = 0.1$, $\chi = 10$, $\bar{r}_0 = 200$, and $\theta_{mac} = 90^\circ$.

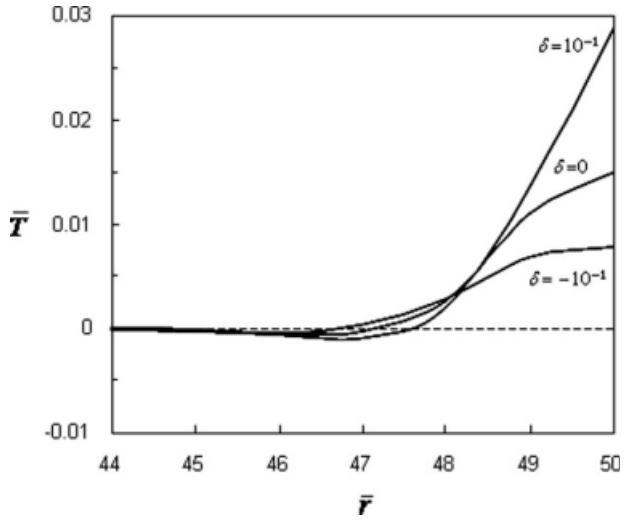

Figure 5. Spatial variation of membrane peeling tension adhered on substrates with linearly increasing ($\delta = 0.01$), decreasing ($\delta = -0.01$), and constant ($\delta = 0$) ligand density.

Parameter values are $\phi = 0.1$, $\varepsilon = 10$, $\omega = 1$, $\chi = 1$, $\bar{r}_0 = 200$, and $\theta_{mac} = 90^\circ$.

receptor density within the adhesion zone and hence, adhesion switches to a receptor-limited regime and bond density reaches a limiting value equal to that of membrane receptor. In Figure 4b, all density profiles abruptly decrease at a narrow boundary layer region close to $\bar{r} = \bar{r}_0$, due to the higher detachment rate of highly stretched marginal bonds (Eq. 3).

The peeling model, as depicted in Figure 1, describes the relative membrane-substrate configuration at the leading edge of an attached cell. To apply this model to the rear edge of the cell, a substrate with negative slope of ligand gradient should be considered. Figure 5 shows the variation of tension along the membrane adhered on substrates with negative and positive gradient slopes, as well as a substrate with uniform ligand density ($\delta = 0$). Tension at the edge of adhesion zone ($T(r_0)$) can be related to the peeling tension according to Eq. 9a. Comparison of the membrane tension values demonstrates that the required peeling tension from substrates with negative slope of ligand gradient, at the rear edge of adhesion zone, is considerably lower than the macroscopic peeling tension from substrates with positive slope of gradient, at the leading edge.

The difference between the required peeling tension at the leading and rear edges of the contact zone provides a driving force for locomotion of motile cells (in the early stages) on ligand gradient substrates. Locomotion can be regarded as a result of two kinetic mechanisms: spreading and peeling, both of which are controlled by the rate of interaction between the membrane and substrate. The higher ligand density at the edge of adhesion zone in the cell front promotes membrane spreading. The rear edge of adhesion zone, which is subjected to a negative slope of ligand gradient, requires a lower tension to detach from the substrate compared with that at the front edge. The asymmetry induced in cell

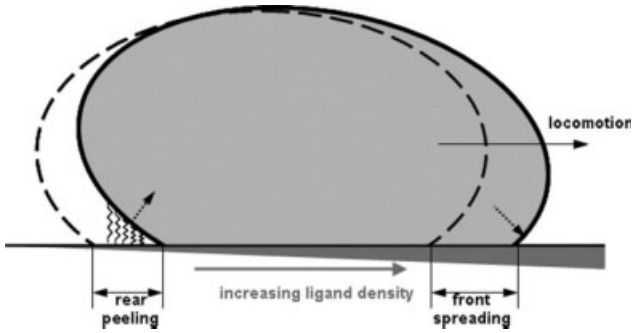

Figure 6. Schematic representation of cell locomotion on a ligand gradient substrate.

Dashed line shows cell configuration before the effect of gradient. Increasing ligand density promotes spreading at the front edge of adhesion zone with lower peeling tension at the rear edge which increases the likelihood of rear detachment. Locomotion takes place toward the direction of increasing ligand density by rear detachment and concurrent front spreading.

configuration by spreading of the front edge increases tension in the membrane, which initiates detachment of highly stretched ligand-receptor bonds at the rear edge of adhesion zone. This effect should be considered along with other proposed mechanisms for rear detachment, such as polarized endocytic trafficking of receptors, contractive force of the cytoskeleton actin filaments, nonuniform thickness of the adhesion zone arising from the diffusion of glycocalyx proteins, focal contact formation of receptors, hydrodynamic pressure gradient across the cell membrane.[40,41] The contribution of contractile force to rear detachment can be included in the proposed model by defining the ligand-receptor equilibrium affinity by $k_{eq} = k_{eq}^0 \exp[-(\kappa l^2 + F\gamma)/2k_B T]$, where F is contractile force and γ is the characteristic length of the binding cleft. Simultaneous rear detachment and front spreading of cell membrane in the adhesion zone induces spontaneous motion of the cell toward the direction of higher ligand density (Figure 6).

Conclusions

We have developed a continuum model to predict the peeling tension of an adherent cell on a solid substrate with a gradient in density of bioadhesive ligands. The ligand density is assumed to increase linearly in a certain direction. The most important prediction of the model is the dependence of peeling tension on the gradient slope and length of adhesion zone. The model predicts that peeling tension increases with gradient slope upto a critical slope above which the adhesion strength is insensitive to ligand gradient. Furthermore, the profile of the membrane in the vicinity of adhesion zone changes significantly with ligand gradient. For substrates with higher gradients, fewer ligand-receptor bonds are stretched at the onset of detachment from the substrate. The model predicts a lower peeling tension and larger number of highly stretched ligand-receptor bonds at the rear edge of the adhesion zone compared with that at the front edge. This indicates that the rupture of ligand-receptor bonds and consequently peeling of the membrane are more likely to be initiated at the rear edge of the adhesion zone.

Acknowledgements

This work was supported by a research grant to E. Jabbari from the National Science Foundation under Grant No. CBET-0756394.

Literature Cited

1. Streuli CH, Bissell MJ. Expression of extracellular matrix components is regulated by substratum. *J Cell Biol.* 1990;111:1405–1415.
2. Hynes RO. Integrins: versatility, modulation, and signaling in cell adhesion. *Cell* 1992;69:11–25.
3. Clark EA, Brugge JS. Integrins and signal transduction pathways: the road taken. *Science* 1995;268:233–239.
4. Huttenlocher A, Ginsberg MH, Horwitz AF. Modulation of cell migration by integrin-mediated cytoskeletal linkages and ligand-binding affinity. *J Cell Biol.* 1996;134:1551–1562.
5. Palecek SP, Huttenlocher A, Horwitz AF, Lauffenburger DA. Physical and biochemical regulation of integrin release during rear detachment of migrating cells. *J Cell Sci.* 1998;111:929–940.
6. Hynes RO, Yamada KM. Fibronectins: multifunctional modular glycoproteins. *J Cell Biol.* 1982;95:369–377.
7. Ruoslahti E, Pierschbacher MD. New perspectives in cell adhesion: RGD and integrins. *Science* 1987;238:491–497.
8. Lauffenburger DA, Linderman JJ. *Receptors: Models for Binding, Trafficking, and Signaling*. New York: Oxford University Press, 1993.
9. Martin JY, Schwartz Z, Hummert TW, Schraub DM, Simpson J, Lankford J, Dean DD, Cochran DL, Boyan BD. Effect of titanium surface roughness on proliferation, differentiation, and protein synthesis of human osteoblast-like cells (MG63). *J Biomed Mater Res.* 1995;29:389–401.
10. Thomas CH, McFarland CD, Jenkins ML, Rezania A, Steele JG, Healy KE. The role of vitronectin in the attachment and spatial distribution of bone-derived cells on materials with patterned surface chemistry. *J Biomed Mater Res.* 1997;37:81–93.
11. Tegoulia VA, Cooper SL. Leukocyte adhesion on model surfaces under flow: effects of surface chemistry, protein adsorption, and shear rate. *J Biomed Mater Res.* 2000;50:291–301.
12. Gumbiner BM. Cell adhesion: the molecular basis of tissue architecture and morphogenesis. *Cell* 1996;84:345–357.
13. Howe A, Aplin AE, Alahari SK, Juliano RL. Integrin signaling and cell growth control. *Curr Opin Cell Biol.* 1998;10:220–231.
14. Hypolite CL, McLernon TL, Adams DN, Chapman KE, Herbert CB, Huang CC, Distefano MD, Hu WS. Formation of microscale gradients of protein using heterobifunctional photolinkers. *Bioconjugate Chem.* 1997;8:658–663.
15. Herbert CB, McLernon TL, Hypolite CL, Adams DN, Pikus L, Huang CC, Fields GB, Letourneau PC, Distefano MD, Hu WS. Micropatterning gradients and controlling surface densities of photoactivatable biomolecules on self-assembled monolayers of oligo(ethylene glycol) alkanethiolates. *Chem Biol.* 1997;4:731–737.
16. Plummer ST, Bohn PW. Spatial dispersion in electrochemically generated surface composition gradients visualized with covalently bound fluorescent nanospheres. *Langmuir* 2002;18:4142–4149.
17. Haddow DB, France RM, Short RD, MacNeil S, Dawson RA, Leggett GJ, Cooper E. Comparison of proliferation and growth of human keratinocytes on plasma copolymers of acrylic acid/1,7-octadiene and self-assembled monolayers. *J Biomed Mater Res.* 1999;47:379–387.
18. Whittle JD, Barton D, Alexander MR, Short RD. A method for the deposition of controllable chemical gradients. *Chem Commun.* 2003;14:1766–1767.
19. Jeon NL, Dertinger SKW, Chiu DT, Choi IS, Stroock AD, Whitesides GM. Generation of solution and surface gradients using microfluidic systems. *Langmuir* 2000;16:8311–8316.
20. Burdick JA, Khademhosseini A, Langer R. Fabrication of gradient hydrogels using a microfluidics/photopolymerization process. *Langmuir* 2004;20:5153–5156.
21. Buck CA. Cell surface receptors for extracellular matrix molecules. *Annu Rev Cell Biol.* 1987;3:179–205.
22. Lanza RP, Langer RS, Chick WL. *Principles of Tissue Engineering*. Austin, TX: Academic Press, 1997.
23. Kang CE, Gemeinhart EJ, Gemeinhart RA. Cellular alignment by grafted adhesion peptide surface density gradients. *J Biomed Mater Res.* 2004;71A:403–411.
24. Bhat RR, Chaney BN, Rowley J, Liebmann-Vinson A, Genzer J. Tailoring cell adhesion using surface-grafted polymer gradient assemblies. *Adv Mater.* 2005;17:2802–2807.
25. Delong SA, Gobin AS, West JL. Covalent immobilization of RGDs on hydrogel surfaces to direct cell alignment and migration. *J Control Release.* 2005;109:139–148.
26. Harris BP, Kutty JK, Fritz EW, Webb CK, Burg KJL, Metters AT. Photopatterned polymer brushes promoting cell adhesion gradients. *Langmuir* 2006;22:4467–4471.
27. Smith JT, Elkin JT, Reichert WM. Directed cell migration on fibronectin gradients: effect of gradient slope. *Exp Cell Res.* 2006;312:2424–2432.
28. Simon KA, Burton EA, Han Y, Li J, Huang A, Luk Y. Enhancing cell adhesion and confinement by gradient nanotopography. *J Am Chem Soc.* 2007;129:4892–4893.
29. Bell GI, Dembo M, Bongrand P. Cell adhesion. *Biophys J.* 1984;45:1051–1064.
30. Evans EA. Detailed mechanics of membrane-membrane adhesion and separation. I. Continuum molecular cross-bridges. *Biophys J.* 1985;48:175–183.

31. Evans EA. Detailed mechanics of membrane-membrane adhesion and separation. II. Discrete kinetically trapped molecular cross-bridges. *Biophys J*. 1985;48:185–192.
32. Zhu C. Kinetics and mechanics of cell adhesion. *J Biomech*. 2000; 33:23–33.
33. Freund LB, Lin Y. The role of binder mobility in spontaneous adhesive contact and implications for cell adhesion. *J Mech Phys Solids*. 2004;52:2455–2472.
34. Sarvestani AS, Jabbari E. Modeling the kinetics of cell membrane spreading on substrates with ligand density gradient. *J Biomech*. 2008;41:921–925.
35. Dembo M, Torney DC, Saxman K, Hammer D. The reaction-limited kinetics of membrane-to-surface adhesion and detachment. *Proc R Soc London B Biol Sci*. 1988;234:55–83.
36. Martinez EJP, Lanir Y, Einav S. Effects of contact-induced membrane stiffening on platelet adhesion. *Biomech Model Mechanobiol*. 2004;2:157–167.
37. Massia SP, Hubbell JA. An RGD spacing of 440 nm is sufficient for integrin $\alpha V\beta 3$-mediated fibroblast spreading and 140 nm for focal contact and stress fiber formation. *J Cell Biol*. 1991;114:1089–1100.
38. Evans EA. Bending elastic modulus of red blood cell membrane derived from buckling instability in micropipet aspiration tests. *Biophys J*. 1983;43:27–30.
39. Guttenberg Z, Lorz B, Sackmann E, Boulbitch A. First-order transition between adhesion states in a system mimicking cell-tissue interaction. *Europhys Lett*. 2001;54:826–832.
40. DiMilla PA, Barbee K, Lauffenburger DA. Mathematical model for the effects of adhesion and mechanics of cell migration speed. *Biophys J*. 1991;60:15–37.
41. Palecek SP, Horwitz AF, Lauffenburger DA. Kinetic model for integrin-mediated adhesion release during cell migration. *Ann Biomed Eng*. 1999;27:219–235.

Manuscript received Jan. 7, 2009, and final revision received Mar. 11, 2009.